assay (*22*). Nonsectoring colonies were isolated, and 28 strains passed tests for dependence on *pGLE1/URA3* and lack of *gle1*Δ alleles. We divided 24 alleles into four complementation groups (Fig. 1A), with 4 remaining unassigned. On the basis of growth defects, the *gsl* alleles were ranked in relative order of increasing severity and penetrance. For characterization experiments, the most severe allele was chosen (for example, *gsl2-6* or *plc1*Δ, *gsl1*Δ, *gsl3-3*, *gle1-4*). Exceptions include the synthetic lethal screen (*gle1-2*) and cloning of *GSL* genes (*gsl1-4*, *gsl2-2*), in which cases the allele used was that most readily complemented by *GLE1* in a colony sectoring assay. Allele-specific differences were noted in the IP profiles of *gsl3-1* and *gsl3-3*, and likely represent distinct mutations.

12. C. A. Saavedra, C. M. Hammell, C. V. Heath, C. N. Cole, *Genes Dev.* **11**, 2845 (1997); F. Stutz *et al.*, *ibid.*, p. 2857.
13. The *plc1* mutant (*gsl2-6*) was also assayed over a time course for poly(A)$^+$ RNA export, and accumulation in some cells was detectable beginning 15 to 30 min after the shift to 37°C. Nuclear protein export was assayed using a green fluorescent protein (GFP) tagged with nuclear localization and export sequences [K. Stade, C. S. Ford, C. Guthrie, K. Weis, *Cell* **90**, 1041 (1997)]. Import assays were performed with a nuclear localization sequence–GFP reporter [N. Shulga *et al.*, *J. Cell Biol.* **135**, 329 (1996)]. Thin-section electron microscopy was performed as described [S. R. Wente and G. Blobel, *ibid.* **123**, 275 (1993)].
14. J. S. Flick and J. Thorner, *Mol. Cell. Biol.* **13**, 5861 (1993).
15. S. Safrany and S. Shears, *EMBO J.* **17**, 1710 (1998).
16. B. Phillippy, A. Ullah, K. Ehrlich, *J. Biol. Chem.* **269**, 28693 (1994).
17. P. Ongusaha, P. Hughes, J. Davey, R. Mitchell, *Biochem. J.* **335**, 671 (1998); F. Estevez, D. Pulford, M. Stark, A. Carter, C. Downes, *ibid.* **302**, 709 (1994).
18. L. Stephens and R. Irvine, *Nature* **326**, 580 (1990).
19. B. Drobak, *Biochem. J.* **288**, 697 (1992); F. Menniti, K. Oliver, J. Putney, S. Shears, *Trends Biochem. Sci.* **18**, 53 (1993).
20. Expression of protein A–tagged Ipk1p on a 2 μm plasmid (with the *GLE1* promoter) complements the synthetic lethality of *gsl1-4 gle1-2* cells and rescues production of IP_6 in *gsl1*Δ cells. Protein A–Ipk1p was not visible when expressed on a centromere plasmid or integrated. In subcellular fractionation experiments, the majority of the centromere expressed protein A–Ipk1p was isolated with nuclei, suggesting the results in Fig. 5 reflect that of endogenous Ipk1p.
21. S. M. Voglmaier *et al.*, *Biochem. Biophys. Res. Commun.* **187**, 158 (1992).
22. R. Murphy, J. L. Watkins, S. R. Wente, *Mol. Biol. Cell* **7**, 1921 (1996).
23. L. E. Stolz, W. J. Kuo, J. Longchamps, M. K. Sekhon, J. D. York, *J. Biol. Chem.* **273**, 11852 (1998).
24. We thank J. Datto for technical help, J. Thorner for sharing unpublished data, and K. Weis and D. Goldfarb for plasmids. Supported by a Burroughs Wellcome Fund Career Award in the Biomedical Sciences (J.D.Y.), a Whitehead Scholar Award (J.D.Y.), Duke University Medical Scientist Training Program (A.R.O.), an NIH Training Grant for predoctoral trainees (R.M. and E.B.I.), and grants from the American Cancer Society (Junior Faculty Research Award) (S.R.W.) and the National Institutes of General Medical Science (S.R.W.).

8 February 1999; accepted 27 May 1999

The Cavity and Pore Helices in the KcsA K^+ Channel: Electrostatic Stabilization of Monovalent Cations

Benoît Roux[1] and Roderick MacKinnon[2]

The electrostatic influence of the central cavity and pore alpha helices in the potassium ion channel from *Streptomyces lividans* (KcsA K^+ channel) was analyzed by solving the finite difference Poisson equation. The cavity and helices overcome the destabilizing influence of the membrane and stabilize a cation at the membrane center. The electrostatic effect of the pore helices is large compared to that described for water-soluble proteins because of the low dielectric membrane environment. The combined contributions of the ion self-energy and the helix electrostatic field give rise to selectivity for monovalent cations in the water-filled cavity. Thus, the K^+ channel uses simple electrostatic principles to solve the fundamental problem of ion destabilization by the cell membrane lipid bilayer.

The cell membrane presents a large energy barrier to ion permeation. Known as the dielectric barrier, this impediment to ion passage is a fundamental property of the low electrical polarizability of the membrane hydrocarbon (*1*). The structure determination of the KcsA K^+ channel shows two unexpected features of its ion conduction pore (*2*). First, at the level of the bilayer center, the pore forms a cavity large enough to contain around 50 water molecules (~5 Å radius), and second, four α helices (pore helices) point their COOH-termini at the cavity center (Fig. 1). It has been proposed that the water-filled cavity and oriented pore helices are the structural basis by which the K^+ channel overcomes the dielectric barrier (*2*).

The K^+ channel not only lowers the dielectric barrier, but it stabilizes a cation near the bilayer center. This conclusion is based on difference Fourier analysis of ion-substituted crystals. When K^+ was substituted with the more electron-dense Rb^+, resulting difference maps showed a positive peak at the cavity center (Fig. 1; red mesh). Further, if the less electron-dense Na^+ is used to substitute K^+, a negative peak is observed (Fig. 1; green mesh). We thus conclude that the cavity is occupied by a cation. In the present theoretical analysis, we investigated whether the cavity and pore helices are sufficient to overcome the dielectric barrier and account for the presence of a cation at the bilayer center.

The electrostatic stabilization of an ion by a water-filled cavity at the membrane center can be understood through a calculation based on the Born theory of solvation (*3*). The free energy for transferring an ion from bulk water into a cavity of radius R and dielectric constant ε_w embedded in a medium of low dielectric constant ε_m is given by

$$\Delta G = (1/2)(Q^2/R)(1/\varepsilon_m - 1/\varepsilon_w) \qquad (1)$$

This equation yields a value of 16.2 kcal/mol for the transfer of K^+ from aqueous solution to a 5 Å (radius) water-filled sphere (ε_w = 80) surrounded by hydrocarbons (ε_m = 2). Transferring the ion from water directly into hydrocarbon (no cavity) would have an energetic cost of more than 60 kcal/mol, and so the cavity will stabilize the ion by more than 40 kcal/mol.

The remaining 16.2 kcal/mol still represents a large energy barrier that precludes the presence of an ion in the cavity. Can the pore helices account for the additional stabilization through the electrostatic field that they impose on their environment (*2, 4*)? According to accepted principles, there are two arguments against this idea. First, the nearest carbonyl oxygen at the COOH-terminus of the helices (Thr^{74}) is 8 Å from the cavity center, whereas electrostatic effects due to α helices are thought to be very small and short range (*5*). Second, the cavity contains about 50 water molecules that would be expected to shield the electric field of the α helix. An α helix in water barely interacts (~−0.14 kcal/mol) with a monovalent cation located 8 Å from its COOH-terminus.

To address the basis of ion stabilization at the center of the KcsA K^+ channel, it is necessary to account for the dielectric shielding in the complex membrane environment. We calculated the electrostatic free energy of a K^+ ion in the center of the cavity, using a macroscopic continuum model of the environment surrounding the KcsA K^+ channel protein. The channel was represented in full atomic detail with all explicit partial charges, whereas the membrane was assigned a dielectric constant of 2 and the water, including the pore and cavity, was assigned a value of 80 (*6*).

[1]GRTM, Dipartements de Physique et Chimie, Université de Montréal, Case Postal 6128, succursale Centre-Ville, Montréal, Canada H3C 3J7. [2]Howard Hughes Medical Institute, Laboratory of Molecular Neurobiology and Biophysics, Rockefeller University, 1230 York Avenue, New York, NY 10021, USA.

To assess the importance of induced electronic polarization and small amplitude librational atomic fluctuations, we carried out the calculation with the internal dielectric constant of the protein ranging between 1 and 5. A dielectric constant of 1 for the interior of the protein provides a direct correspondence with the force field in which the atomic partial charges are present explicitly; values of 2 to 5 examine the importance of induced electronic polarization and small-amplitude librational atomic fluctuations (*7*).

To first assess the influence of the irregular shape of the protein and the presence of the membrane interface, we calculated the free energy of transfer of one K^+ ion into the center of the cavity while all the charges in the system were turned off (Fig. 2, circles). This calculation yielded the charging free energy contribution arising from the interaction of the ion with its own reaction field (the self-energy), a quantity corresponding conceptually to a Born charging energy, as given in Eq. 1, but taking into account the detailed molecular shape of the membrane channel system. Because of the uncertainty of the protein dielectric constant, the calculation was carried out for values from 1 to 5. For a protein dielectric constant of 2, the calculated free energy of transfer is 6.3 kcal/mol. This energy is smaller than predicted by Eq. 1 (16.2 kcal/mol) because the true shape of the cavity is not a sphere and because the bulk water interfaces are not infinitely far away. The square symbols (Fig. 2) show the much larger energies that would result if the cavity were absent (that is, if it were filled with weakly polar material of dielectric constant = 2), emphasizing the energetic stabilization brought about by the presence of the water-filled cavity.

We then restricted the calculations to the case where the protein dielectric constant is set at a value of 2, although further calculations have shown that the conclusions reached are not affected qualitatively by this choice. To assess individual contributions to ion stabilization in the cavity, we calculated the free energy of ion transfer while turning on various charges in the system. The presence of two K^+ ions in the selectivity filter increases the transfer energy of an ion (from water to the cavity) from 6.3 kcal/mol to 16.3 kcal/mol as a result of ion repulsion (Table 1). However, the transfer energy drops to –8.5 kcal/mol when all the atomic charges of the protein are turned on (in the presence of the selectivity filter ions). Eighty percent of the stabilization by the protein results from the pore helices, consisting of only 13 amino acids per subunit, and therefore their precise orientation with respect to the cavity center is crucial. The remaining stabilization due to the protein results mainly from the carbonyl of Thr^{75}. Although the carbonyl (one from each subunit) is involved in the coordination of one K^+ ion in the selectivity filter, it is roughly 8 Å from the cavity center and contributes about –5 kcal/mol.

The origin of the electrostatic stabilization due to the pore helix is shown in Fig. 3. If one imagines building the helix starting at its COOH-terminal extent and working backward one residue at a time, most of its effect results from the amide-carbonyl dipoles of the first five amino acids. However, residues even further away contribute to some extent (circles). Why—in contrast to conclusions reached on the basis of studies of water-soluble proteins—do the pore helices have such a large electrostatic effect? Because electric fields are less shielded in the low dielectric membrane environment. This can be seen by setting the membrane dielectric constant to a value of 80 as if the channel were a soluble protein: In this case, all the energies are attenuated (Table 1). Thus, the low dielectric membrane environment con-

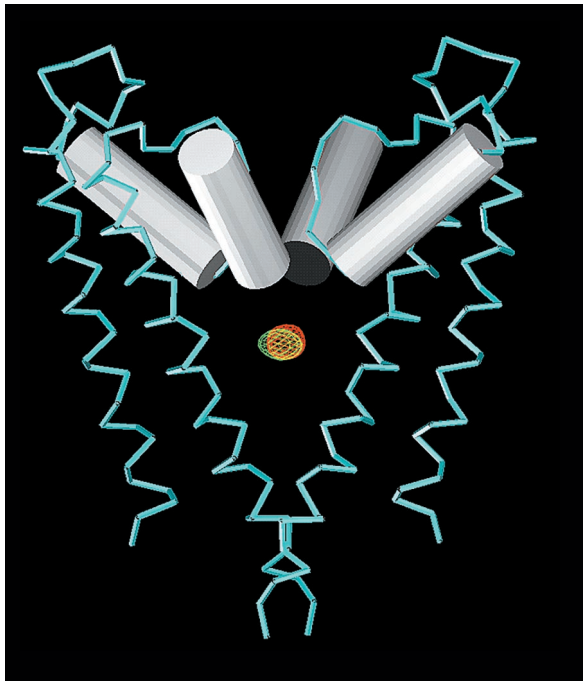

Fig. 1. Picture of the KcsA K^+ channel structure showing the main-chain trace from two subunits (cyan) and the pore helices from all four subunits (white cylinders). The pore helices are directed with their COOH-terminus pointed at the membrane center where a water-filled cavity is located. The extracellular and intracellular sides of the channel are on the top and bottom, respectively. Positive electron density is present at the cavity center on difference Fourier maps when K^+ in the native crystal is substituted with Rb^+ (red mesh). A negative peak in the cavity is observed when less electron-dense Na^+ is the replacement ion (green mesh; superposition of red and green gives yellow). The difference maps were calculated using Fourier coefficients F(soak) – F(native) and multiple isomorphous replacement, solvent-flattened, averaged phases and contoured at 7.0 σ (root mean square deviation) and –6.0 σ for the Rb^+ and Na^+ difference maps, respectively (*13*).

Table 1. Calculated free energy (in kilocalories per mole) for the transfer of a single K^+ ion from bulk water to the cavity center is shown for a variety of conditions. K^+_1 refers to the ion being transferred into the cavity, whereas K^+_2 and K^+_3 refer to the ions in the selectivity filter. The pore helix consists of residues Tyr^{62} to Thr^{74} in addition to the main-chain atoms of Thr^{75}, but excluding its carbonyl group. The side chain of Glu^{71} has been modeled in its protonated state. "All protein" and "pore helices only" refer to the part of the protein where charges have been turned on.

	K^+_1 only	K^+_1, K^+_2, K^+_3 only	K^+_1, K^+_2, K^+_3 and all protein	K^+_1, K^+_2, K^+_3 and pore helices only
KcsA embedded in membrane	6.3	16.3	−8.5	−4.5
KcsA in bulk water solution	2.1	5.9	−3.4	−1.4

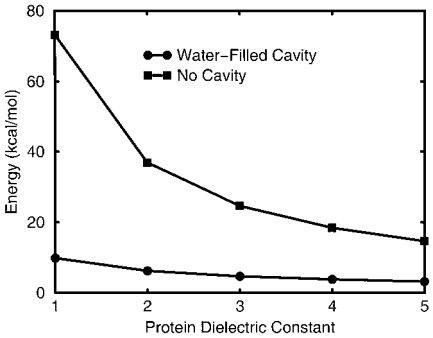

Fig. 2. Born free energy of K^+ ion transfer from bulk water to the center of the cavity in the KcsA K^+ channel. Full finite difference Poisson calculation for the KcsA K^+ channel with the dielectric constant of bulk water assigned for the interior of the cavity (circles) or when the cavity is assigned the same dielectric constant as the remainder of the protein (squares). Energy is plotted as a function of protein dielectric constant for values from 1 to 5. All charges other than the K^+ in the center of the cavity are turned off.

tributes significantly to amplifying the magnitude of cation stabilization by the pore helices. Our calculations were made using a value of 25 Å for the membrane thickness. The relative stabilization conferred by the pore helices would increase even further in the case of a thicker membrane.

The water-filled cavity does not completely shield the field of the pore helix. By comparing the helix effect on the ion transfer energy in the case of the channel (Fig. 3, circles) versus a uniform dielectric constant of 2 (squares), we see that the water outside the membrane and in the cavity adds an offset to the energy curve. However, the remaining effect due to the helix is still large compared to the case of a uniform dielectric of 80 (triangles). The "energy well" produced by the combination of the water-filled cavity and pore helices is quite uniform over much of the axial length of the cavity. That is, the energy for transferring a K^+ ion from water to different locations along the pore axis between −4 Å and 4 Å, relative to zero at the cavity center, is similar. In contrast, only off-axis lateral displacements on the order of 2 Å are energetically allowed. This suggests that, despite the stabilizing electrostatic energy, the structure of the K^+ channel is designed to keep the ion focused in the center of the cavity without preventing rapid transport.

Electrostatic stabilization of an ion can be decomposed into reaction field and static field contributions. The general solution for the electrostatic Gibbs free energy for transferring an ion of charge Q into an inhomogeneous medium with dielectric boundaries and static charges may be expressed as

$$\Delta G(Q) = (1/2)AQ^2 + BQ + C \qquad (2)$$

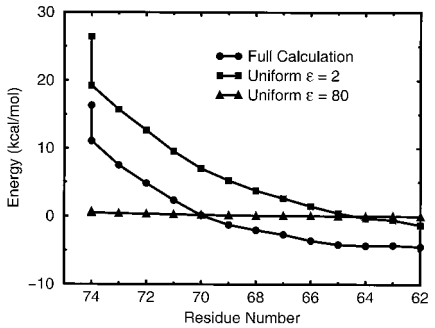

Fig. 3. Stabilization of a K^+ ion in the center of the cavity as a result of the electric field of the pore helix backbone. The first point (residue 74) indicates the initial energy with zero helix contribution and subsequent points correspond to addition of sequential amide-carbonyl groups from the pore helix residues. The contribution due to the C=O group of Tyr^{62} through the C=O group of Thr^{74} (and the N–H of Thr^{75}) corresponds to the full finite difference Poisson calculation (circles). The result for a simple coulomb law calculation, assuming a uniform dielectric constant of $\varepsilon = 2$ (squares) and $\varepsilon = 80$ (triangles), is shown for comparison.

where A is the reaction field term, B is the static field term, and C is a constant term due to the influence of the dielectric constant of the ion on the protein charges (C is negligibly small). The reaction field is always destabilizing, whereas the static field is cation-attractive because of the pore helices. Our calculations allow us to evaluate the constants $A = 12.5$, $B = -14.9$, and $C = 0.1$. In the case of a divalent cation ($Q = 2$) the transfer free energy is −4.6 kcal/mol, significantly less favorable than for a monovalent cation. The optimal charge for which the transfer is most favorable is $-B/A = +1.2$ unit charge. Thus, the KcsA K^+ channel is tuned to preferably stabilize a monovalent cation at the center of the membrane. The biological utility of such tuning is evident. The K^+ selectivity filter is located at the extracellular third of the pore, and therefore, cations other than K^+ should be able to enter from the cytoplasm, penetrate two-thirds of the way across the membrane, and clog the pore at the selectivity filter. The valence selectivity of the cavity will favor monovalent cations over intracellular polyvalent cations such as Mg^{2+} and polyamines. The abundance of K^+ compared to Na^+ inside the cell will ensure that the monovalent cation in the cavity is predominantly K^+.

One class of K^+ channels, known as inward rectifiers, is susceptible to blocking by cytoplasmic polyvalent cations; consequently, when the electrochemical driving force for K^+ favors flow outward across the cell membrane, the pore of these channels becomes occluded. This property is central to the operation of inward-rectifier K^+ channels. It turns out that these K^+ channels have a polar residue (Asn or Asp) at the position of an amino acid that lines the wall of the cavity (*8*). In other words, the inward-rectifier K^+ channels have a modified static field—they are tuned for multivalent cations. Likewise, we anticipate that Ca^{2+} channels will have pores that are related architecturally to K^+ channels and wait to see if they will be electrostatically optimized to stabilize a Ca^{2+} ion in the membrane center, beneath their selectivity filter.

A complete description of ion conduction and selectivity in a K^+ channel, a multi-ion pore, will require a detailed account of ion-ion and ion-protein energetics and dynamics. It has been long recognized that a primary role of any ion channel is to overcome the dielectric barrier presented by the cell membrane (*1*). We show that the KcsA K^+ channel makes use of simple electrostatic principles to overcome the barrier, and anticipate that these principles will apply to other biological transport systems. Our conclusions are summarized as follows: (i) A water-filled cavity at the center of the membrane contributes significantly to the stabilization of ions. (ii) A static field attributed largely to specifically oriented α helices stabilizes a positive ion. (iii) The electrostatic effect of the helices is large compared to that described for water-soluble proteins because of the low dielectric membrane environment. (iv) The ion is focused along the pore axis, but the "energy well" is broad. These properties favor a high ion throughput. (v) The combined contributions of the reaction and static fields result in monovalent cation selectivity.

References and Notes

1. A. Parsegian, *Nature* **221**, 844 (1969).
2. D. A. Doyle *et al.*, *Science* **280**, 69 (1998).
3. M. Born, *Z. Phys.* **1**, 45 (1920).
4. W. G. J. Hol, P. T. van Duijnen, H. J. C. Berendsen, *Nature* **273**, 5662 (1978); W. G. J. Hol, *Prog. Biophys. Mol. Biol.* **45**, 149 (1985).
5. J. J. He and F. A. Quicho, *Protein Sci.* **2**, 1643 (1993).
6. Atomic partial charges were taken from the all-hydrogen PARM22 potential function (*9*) of CHARMM (*10*). The dielectric boundary between the protein and environment was constructed on the basis of a set of atomic Born radii derived from the average solvent radial charge distribution functions around the 20 amino acids in molecular dynamics simulations with explicit water molecules (*11*). The complete system was mapped onto a cubic grid, and the Poisson equation was solved numerically. No electrolyte was included in the bulk solution. The total electrostatic potential was calculated at each point of the grid by solving the finite difference Poisson equation. The numerical calculations were carried out using the standard relaxation algorithm (*12*). The calculation was done in two steps, first using a grid spacing of 1.0 Å (130^3 points, with periodic boundary conditions in the membrane plane), followed by a focusing around the main region with a grid spacing of 0.5 Å. The free energy of transfer of a K^+ ion from the aqueous solution to the center of the cavity of the KcsA channel was calculated as one-half times the electrostatic energy of the channel containing the cavity ion minus the electrostatic energy of the channel without the ion and minus the electrostatic energy of the ion in bulk water.
7. T. Simonson and C. L. Brooks, *J. Am. Chem. Soc.* **118**, 8452 (1996).
8. Z. Lu and R. MacKinnon, *Nature* **371**, 243 (1994); B. A. Wibble, M. Taglialatela, E. Ficker, A. M. Brown, *ibid.*, p. 246; A. N. Lopatin, E. N. Makhina, C. G. Nichols, *ibid.* **372**, 366 (1994).
9. A. D. Mackerell *et al.*, *J. Phys. Chem. B* **102**, 3586 (1998).
10. B. R. Brooks *et al.*, *J. Comput. Chem.* **4**, 187 (1983).
11. M. Nina, D. Beglov, B. Roux, *J. Phys. Chem. B* **101**, 5239 (1997).
12. J. Warwicker and H. C. Watson, *J. Mol. Biol.* **157**, 671 (1982); I. Klapper, R. Hagstrom, R. Fine, K. Sharp, B. Honig, *Proteins* **1**, 47 (1986).
13. Crystals of the KcsA K^+ channel were prepared by mixing equal volumes of protein solution [KcsA K^+ channel (5 to 10 mg/ml), 150 mM KCl, 50 mM tris (pH 7.5), 2 mM dithiothreitol, and 5 mM *N*,*N*-dimethyldodecylamine-*N*-oxide (LDAO)] with reservoir solution [200 mM $CaCl_2$, 100 mM Hepes (pH 7.5), and 48% PEG-400] as described (*2*). Exchange of ions in the pore was accomplished by replacing the 150 mM KCl with 150 mM RbCl or NaCl. Crystals were frozen at liquid nitrogen temperature and data was collected at the Cornell High Energy Synchrotron Source (CHESS) A1 station. Data were processed using Denzo and Scalepack [Z. Otwinowski, in *Data Collection and Processing*, L. Sawyer and S. Bailey, Eds. (Science and Engineering Research Council Daresbury Laboratory, Daresbury, UK, 1993), pp. 56–62] and CCP4 programs [Collaborative Computation Project 4 (CCP4), *Acta Crystallogr. D* **50**, 760 (1994)]. Difference maps were calculated with data to 4.0 and 5.0 Å for Rb^+ and Na^+, respectively.

14. Supported by the Medical Research Council of Canada grant MT-11538 to B.R. and by NIH grant GM47400 to R.M. R.M. is an investigator in the Howard Hughes Medical Institute.

22 December 1998; accepted 20 April 1999